Available online at www.sciencedirect.com
ScienceDirect
Journal of the European Ceramic Society 28 (2008) 149–157
www.elsevier.com/locate/jeurceramsoc

Manufacture of macroporous β-tricalcium phosphate bioceramics

M. Descamps [a,*], T. Duhoo [b], F. Monchau [a], J. Lu [c], P. Hardouin [c], J.C. Hornez [a], A. Leriche [a]

[a] *Laboratoire des Matériaux et Procédés (LMP), EA 2443, Université de Valenciennes et du Hainaut-Cambrésis, ZI du champ de l'Abbesse, 59600 Maubeuge, France*
[b] *Laboratoire de Structure et Propriétés de l'Etat Solide (LSPES), UMR 8008, Université des Sciences et Technologies de Lille, Bâtiment C6, 59655 Villeneuve d'Ascq, France*
[c] *Laboratoire de Recherche sur les Biomatériaux et les Biotechnologies (LR2B-LBCM), UPRES EA 2603 IFR 114, Université du littoral et cote d'opale, Boulogne, France*

Received 6 April 2007; accepted 13 May 2007
Available online 17 September 2007

Abstract

β-Tricalcium phosphate (β-TCP) macroporous ceramics were produced by a new manufacturing procedure. An organic skeleton constituted of polymethylmethacrylate balls (PMMA) is carried by a chemical forming treatment. This treatment consists to establish a connection between PMMA balls by a chemical superficial dissolution of the individual beads. This reaction is accompanied of significant shrinkage of the organic skeleton which is correlated with the interconnection size between beads.

An empirical relation and a geometrical model, based on a theoretical arrangement of spheres of uniform sizes, were developed to determine the necessary shrinkage of the organic skeleton to obtain a desired interconnection size.

PMMA skeleton is impregnated by using an aqueous suspension of β-TCP, after drying, the ceramic/polymeric composite undergoes the traditional steps of debinding and sintering to obtain finished material.

This process allows a total control of the porous architecture of the part (sizes of pores and interconnections) and also to perform materials with very varied forms and dimensions with specific properties as a gradient of pore sizes or a gradient of the interconnection sizes.

Keywords: Biomedical applications; β-Tricalcium phosphate (TCP); Porosity; Slip casting

1. Introduction

Ceramic materials used for to repair and reconstruction of damaged parts of the human skeleton must present many properties.[1] Ideal biomaterial must be biocompatible, bioactive, resorbable, osteoconductor, osteoinductor, have good mechanical properties and to be available in unlimited quantity.[2] The majority of these properties are primarily dependent on the chemical composition and the porous architectural characteristics of the implant. Among bioceramics used in this field (alumina, zirconia, calcium sulphate, calcium carbonate, etc.), calcium phosphates and in particular hydroxyapatite (HA)[3] and β-tricalcium phosphate (β-TCP)[4] have a place of choice in the clinical practice for a long time. Their chemical compositions, near of the bone, confer them excellent biological properties. These products are used in a pure state or in the form of a biphasic mixture with variable proportions.[5] Moreover, the resorbability of β-TCP allows a gradual biological degradation over a period time and a progressive replacement by the natural host tissue.[6,7] So, β-TCP is currently considered as a very interesting material for bone reconstruction and is frequently used for bone to repair in the form of ceramic blocks, granules and calcium phosphate cements.

The osteoconduction of the implant, i.e. the colonisation of material by new bone, is ensured by the porous structure of material. In this manner, the porous implant establishes a stable interface with connective tissues and serves a scaffold for bone formation and colonisation. To favour cellular and vascular penetration which ensures bone ingrowth inside pores, the porous architecture of material must be perfectly controlled and in particular the dimension of the pores and interconnections between pores.

* Corresponding author.
E-mail address: michel.descamps@univ-valenciennes.fr (M. Descamps).

0955-2219/$ – see front matter © 2007 Elsevier Ltd. All rights reserved.
doi:10.1016/j.jeurceramsoc.2007.05.025

In spite of many researches, ideal pore structure is difficult to determine. Indeed, the investigations were carried out on materials presenting of the very diverse porous characteristics (geometry and surface roughness of the pores, porous volume value) and different resorption rates. Moreover, the sites and times of implantation of these implants also are very varied. Nevertheless, most studies suggested that cell colonisation and bone ingrowth apparently occur if macropore size is greater than 100–150 μm[8–12] and if interconnectivity is greater than 50.[13]

A precise control of scaffold porosity and internal pore structures parameters is thus essential for the therapeutic effectiveness of the implant.

The synthetic ways to manufacture a macroporous material include polymer porosifier method,[14–16] foaming method,[17,18] solid reaction method,[19,20] replicas of porous structure[21,22] and prototype 3D.[23]

This study focused on a new manufacture process of macroporous β-tricalcium phosphate bioceramics.which uses slip casting shaping and polymethylmethacrylate (PMMA) as porogen agent and allows a significant control of the porous structure.

2. Experimental procedure

Polymethylmethacrylate (PMMA) balls with a fixed granulometric distribution are chemically stuck together in order to manufacture an organic scaffold in the shape of a block. This chemical welding or chemical forming is ensured by a solvent which causes a slow superficial dissolution of polymer and allows the realisation of bridges at the contact points between balls.

Voids between polymeric particles are then filled by an aqueous calcium phosphate suspension. After drying of sample in a plaster mould, a debinding treatment, carried out at low temperature, allows to eliminate the porogen agent (PMMA) and to create the macroporosity within ceramic. Bridging between PMMA balls will generate multiple interconnections between pores of sintered body with dimensions equivalent to the size of these bridges. After this debinding stage, the sintering allows to consolidate ceramic walls limiting the pores.

The different steps of macroporous ceramic manufacturing are represented on Fig. 1.

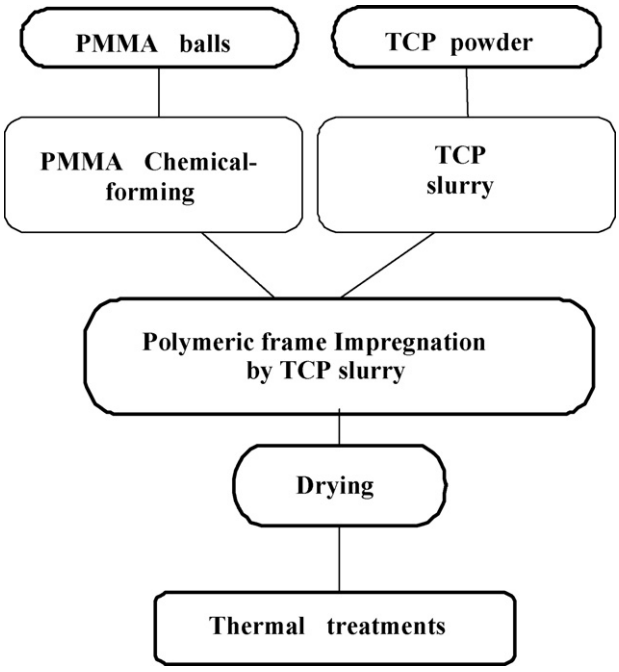

Fig. 1. Synoptic for the manufacture of macroporous body.

2.1. Manufacturing of organic frame

2.1.1. Porogen choice

The PMMA was selected to construct the polymeric frame (Diakon ™ Ineos Acrylics, Holland). This polymer presents an easy and clean thermal elimination and especially a significant chemical dissolution with many solvents.

A spherical shape of this agent was selected in order to allow the control of the dimension, the morphology and the homogeneity of polymeric frame. Chemical-forming trials were performed on balls with diameters in the range of 100–800 μm, obtained by mechanical sieving.

2.1.2. Chemical forming process

The connection between PMMA balls is carried out by a chemical treatment. To produce these bridging, a solvent is carefully poured over a dense pile of spherical bodies, contained in a metallic mould. This solvent must have a dissolution chemical action with respect to the PMMA. Among the numerous traditional solvents usable, the choice was made on aceton (RPE 99.8% Carlo Erba, France). This solvent slowly dissolves parts of the bodies and induces an overlapping between the individual bodies. This movement leads to the formation of necks between PMMA balls and a significant shrinkage of the ball pile.

The neck size is influenced by numerous parameters such as: the chemical nature of solvent and the quantity poured on the balls pile, the dissolution duration, the trial temperature, the load on ball pile. In order to control the neck dimension between balls, independently of all these factors, the dimensional variation of the organic frame is recorded continuously during the chemical forming treatment then to correlate with the interconnection size between beads.

To measure the shrinkage of the organic scaffold, caused by the PMMA ball coalescence, a piston precisely sliding in the metal mould is put in contact to the surface of the bed of balls, in its highest part. On the top of the piston, an electronic displacement sensor is positioned, with a resolution to one micrometer (Tesa Digico 11 Tesa, France), which records the movement of polymeric material according to z direction.

For different shrinkages, the chemical dissolution or bridging between balls is stopped by water action and the neck diameter is evaluated by a Scanning Electron Microscope (Hitachi S-3500N).

These trials allowed to establish a relation between the shrinkage of polymeric frame and the ball connection size.

2.2. Impregnation of the organic frame

The impregnation of PMMA skeleton is carried out by using an aqueous suspension of β-TCP. This stage required: (i) the synthesis of the β-tricalcium phosphate powder with granular characteristics and a chemical composition adapted to a correct setting in suspension of the powder and to an important densification of material and (ii) the optimisation of the casting suspension.

2.2.1. Synthesis and characterisation of β-TCP powder

Stoichiometric β-TCP powder was prepared by aqueous precipitation technique using a diammonium phosphate solution $(NH_4)_2HPO_4$ (Carlo Erba, France) and a calcium nitrate solution $Ca(NO_3)_2{\cdot}4H_2O$ (Brenntag, France).

The solution pH was adjusted at a constant value of 6.5 by a continuous addition of ammonium hydroxide. Temperature was fixed to 30 °C and the solution was matured 24 h. After ripening, solution was filtered and the precipitate was dried to 80 °C. After calcination at 900 °C, powder was ground to break up agglomerates formed during the calcinations. This grinding step was carried out by ball milling with HDPE milling jar and Yttrium Stabilised Zirconia grinding medias during 3 h. After this treatment, specific surface area of ground powders recorded by the BET method (Micromeritics, Flow Sorb 3) was equal to 5.2 m^2/g.

A preceding work[24] showed that it was preferable to use composition with a Ca/P ratio slightly higher than 1.5. Indeed, the presence of the hydroxyapatite phase inhibits the particle enlargement and thus, allows a better densification of part. Thus, the amount of initial reagents were selected in order to obtain final powder slightly over stoichiometry and containing 2 wt.% of HA. Quantitative analysis was performed by Powder X-Ray Diffraction analysis (Rigaku Miniflex) using the intensity ratio of lines $I_{HA(211)}/I_{TCP(0210)}$ in according to method of the proportioned addition.[25,26] The XRD spectra were collected employing a step width of 0.02° with counting time fixed to 20 s under 30 kV and 15 mA exciting (Fig. 2).

2.2.2. Slip preparation and manufacturing ceramics

β-TCP aqueous slurries were prepared with a powder concentration varying from 60 to 65 wt.% according to the density of the PMMA skeleton.

Slurry defloculation is assured by a commercial organic agent (Darvan C, R.t. Vanderbilt Co.) in amount equals to 1.5 wt.% of β-TCP content. A quantity of organic binder (4 wt.% of TCP content, Duramax B1001, Rohm and Haas) was added to ensure a consolidation of green material during the debinding treatment. After a planetary milling during 1 h using agate grinding container and balls, the slurry was poured into plaster mould containing the polymeric frame. The plaster mould ensures the drying of material.

2.3. Thermal treatments

The PMMA elimination is carried out by a thermal treatment at low temperature. A heating to 220 °C during 30 h allows to burn a large quantity of polymer. The residual organic is then eliminated during a heating at 400 °C during 5 h. After this debinding treatment, samples are sintered at 1115 °C during 3 h in order to consolidate the ceramics. This treatment allow to reach a relative density equal or higher than 99%.

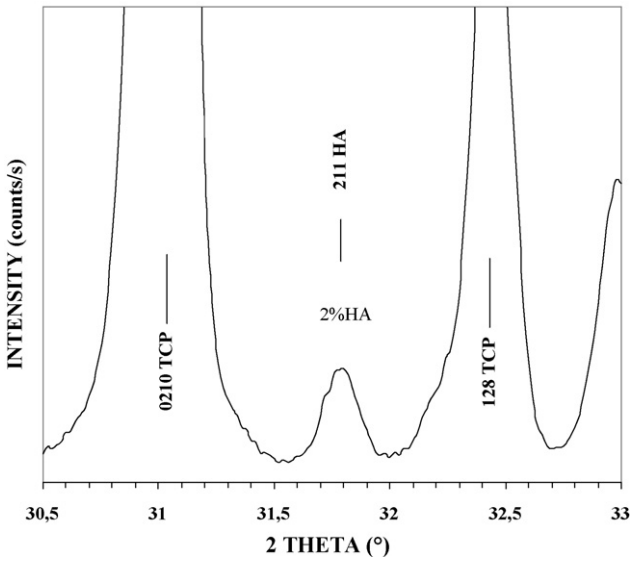

Fig. 2. XRD pattern of TCP powder.

3. Results and discussion

3.1. Chemical forming of PMMA balls

3.1.1. Empirical study

The bridging or chemical welding of polymethylmethacrylate, balls evaluated by the fracture facies and according to the shrinkage of organic frame, is shown in Fig. 3.

This experimentation is carried out at room temperature with granulometric distribution of balls varying from 400 to 500 μm. The treatment duration varies from 30 min to 2 h and the shrinkage of organic frame evolves between 190 and 3800 μm, respectively. The initial height of samples was about 23 mm. These micrographies indicate many contact points between balls and a spherically of the polymeric bead preserved. The connection size increases significantly with the increasing of the organic skeleton shrinkage. The large interpenetrating of balls involves a reduction in the voids between balls. This behaviour permits to obtain very high interconnection sizes between pores and an increase of the porous volume of sintered material. However, too high densities of the organic skeleton generate difficulties during the impregnation of the organic edifice by the casting slurry.

The overlapping progress with time of spherical particles is followed by measuring the diameter of the contact circle, as a function of shrinkage of organic frame (Δ). Fig. 4 shows this evolution performed with three granulometric distribution, as 200–300, 400–500 and 600–700 μm. The precision obtained on the interconnection size is estimated to 10%. In order not to be dependent on the initial height H of the organic frame, the curves are traced according to Δ/H.

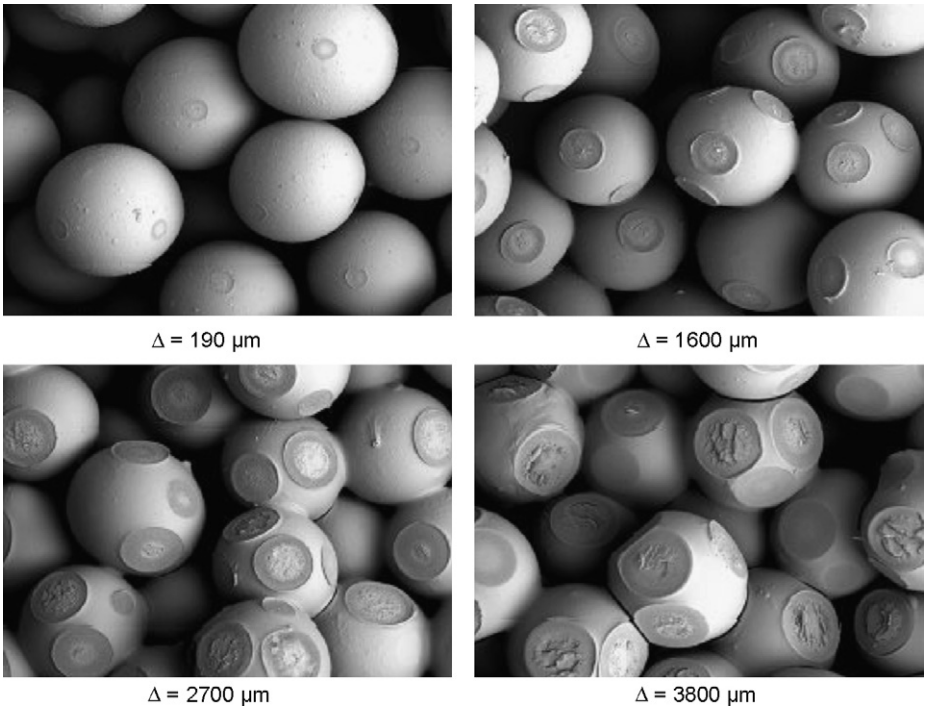

Fig. 3. Evolution of interconnection sizes in according to the shrinkage of organic frame.

These curves were fitted by a linear evolution with mathematical forms following:

$$\text{Balls } 200\text{–}300\,\mu\text{m}, \quad \phi = 541\frac{\Delta}{H} + 49.64$$

$$\text{Balls } 400\text{–}500\,\mu\text{m}, \quad \phi = 1370\frac{\Delta}{H} + 81.84$$

$$\text{Balls } 600\text{–}700\,\mu\text{m}, \quad \phi = 2130\frac{\Delta}{H} + 134.5$$

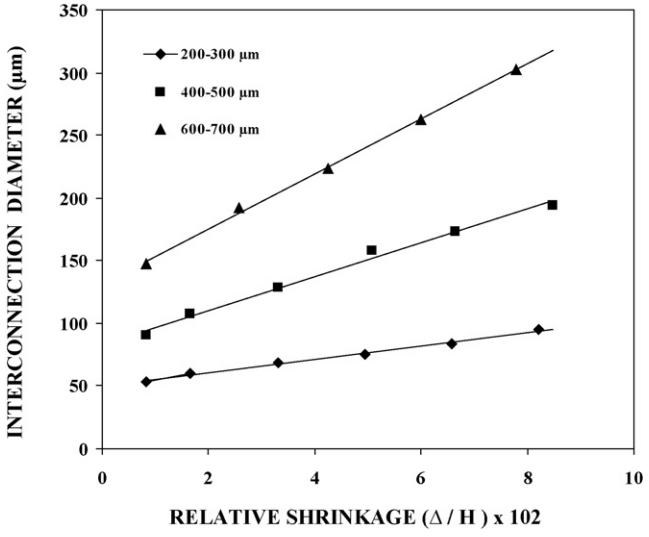

Fig. 4. Interconnection size as a function of relative shrinkage of organic skeleton.

These empirical relations allow to determine the necessary shrinkage of the organic skeleton to obtain a desired interconnection diameter.

3.1.2. Geometrical model

A geometrical model, based on a theoretical arrangement of uniform sized spheres was developed to mathematically calculate the shrinkage according to the diameter of interconnection between PMMA balls.

The arrangement of any particles of diameter $2r$ may be packed into several geometric arrays. A frequently cited model proposes a theoretical arrangement according to five different packing structure.[27] Table 1 summarizes these various models with the shear angle for cubic face and the calculated relative density associated to each unit cell.

Many authors were interested in the determining density of monosphere packing.[28–30] All conclude that the average packing efficiency of monospheres is about 59%, independently of the size and density of material used and for a loose random packing (i.e. in the absence of external forces). In our study, the measurements, carried out on raw pile of PMMA balls with dif-

Table 1
Packing arrays for uniform spheres

	Shear angles (°)			Relative density (%)
	Base	Front	Side	
Cubic	90	90	90	52.36
Simple stagger	90	60	90	60.46
Double stagger	90	60	60	69.81
Pyramidal	90	45	45	74.04
Tetrahedral	60	60	60	74.04

Table 2
Relative density for a loose random packing of PMMA beads

Diameter balls (μm)	Relative density (%)
200–300	58.9
300–400	59.5
400–500	59.4
500–600	59.8
600–700	60.1

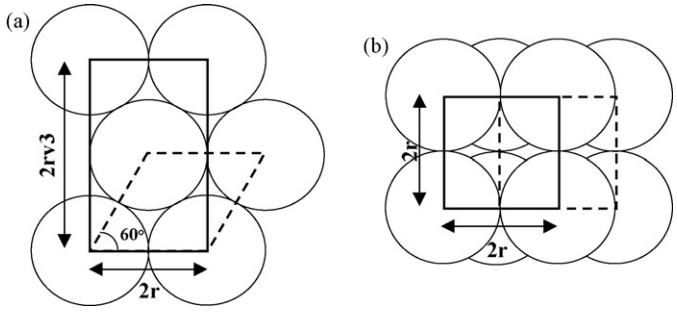

Fig. 5. Vertical (a) and horizontal (b) cross sections of stacked spheres in a simple stagger packing structure (before chemical forming). Representation of the chosen lattice for discussion whereas the primitive lattice is in dashed line (the angle of sheared square is equal to 60°).

ferent granulometric distributions, reveal a density varying from 59 to 60% (Table 2). This density is analogous to the simple stagger structure.(Fig. 5). This arrangement was thus selected for the model study.

In this work, we propose a simple model based on isotropic interconnection between spheres initially in contact. Fig. 6 provides us, by geometrical consideration, the interconnection diameter Φ given by

$$\Phi = 2\sqrt{r^2 - (r - dr)^2} = 2r\sqrt{1 - \left(1 - \frac{dr}{r}\right)^2} \quad (1)$$

where dr is the value of each sphere displacement. We can easily express dr from the shrinkage Δ and the initial height H of sample. For that, H can be written like a multiple of lattice parameter (see Fig. 5):

$$H = N2r\sqrt{3} \quad (2)$$

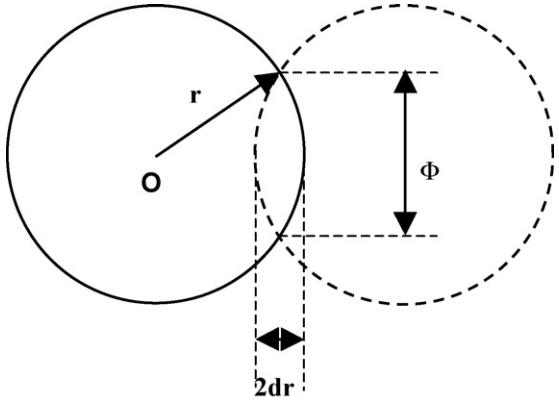

Fig. 6. Interconnection diameter representation with the elementary displacement dr of two r radius spheres.

where N is the number of unit cell in the shrinkage direction. The shrinkage per cell is given by

$$dz = \frac{\Delta}{N}\frac{\Delta 2r\sqrt{3}}{H} \quad (3)$$

Figs. 5 and 6 provide us the following relation:

$$dz = 2dr\sqrt{3} \quad (4)$$

By a combination of Eqs. (3) and (4), we finally obtain:

$$\frac{dr}{r} = \frac{\Delta}{H} \quad (5)$$

The Eq. (1) becomes:

$$\Phi = 2r\sqrt{1 - \left(1 - \frac{\Delta}{H}\right)^2} \quad (6)$$

We can easily remark that we would obtain the same form of Eq. (5) for others structures such: simple cubic, body-centred cubic, face centred cubic. Therefore the model presented for the simple stagger structure is independent from the initial orientation of sample.

The maximum of sphere displacement is obtained as soon as a sphere is in contact with two others. For the simple stagger structure the limitation of our model is given by the following relation:

$$\frac{dr}{r} \leq 1 - \frac{\sqrt{3}}{2} \approx 0.134 \quad (7)$$

We can easily remark in the bottom figure that the maximum density is not reached for this value (Fig. 7) and the maximum value for the interconnection diameter is equal to r. Furthermore, the relation (7) provides us an indication of the maximum shrinkage value used in the experiments. This value cannot exceed 13.4% initial height of the ball pile.

Fig. 8 shows the interconnection diameter Φ versus the shrinkage Δ determined by empirical study and calculated by the geometrical model, for different sphere diameters. For each experiment, the initial height of pile balls was for beads size of 200–300, 300–400, 400–500, 500–600 and 600–700 μm equal

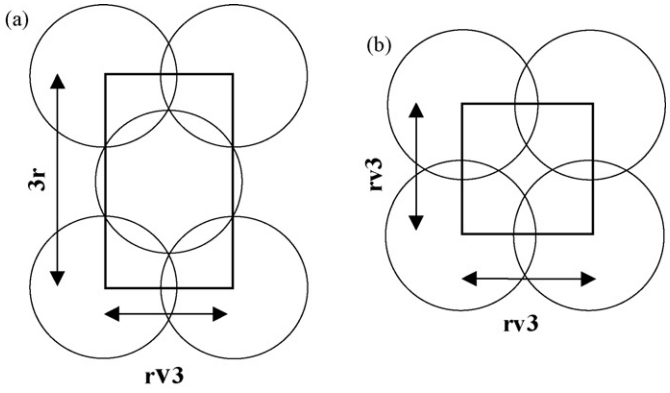

Fig. 7. Vertical (a) and horizontal (b) cross section of stacked spheres in a simple stagger packing structure (after chemical forming).

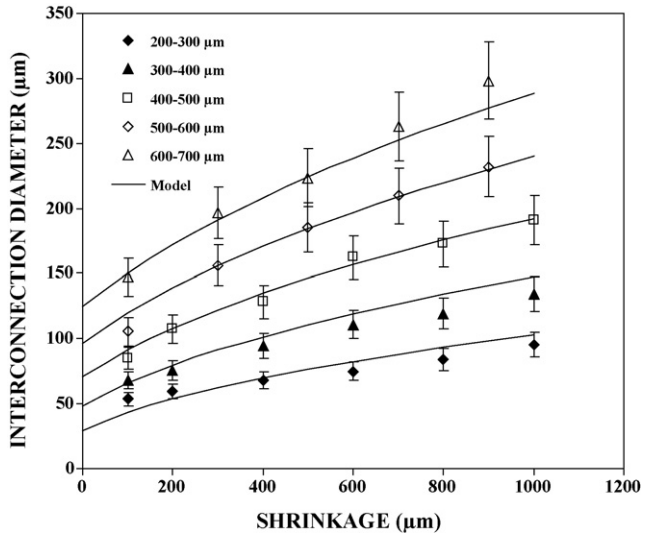

Fig. 8. Comparison between empirical study and model.

to 12.13, 12.03, 11.97, 11.8 and 11.7 mm, respectively. The relative experimental incertitude is estimated at 10% and represented by the error bars.

We needed to add a constant in Eq. (6) to reproduce the experimental behaviour for which the interconnection diameter is not equal to zero at the beginning of chemical forming. This can easily be explained by an initial residual stress in the sample. The formula applied for all the experiments is given by Eq. (8):

$$\Phi = 2\bar{r}\sqrt{1-\left(1-\frac{\Delta}{H}-\frac{2\bar{r}}{3H}\right)^2} \tag{8}$$

where $\bar{r}$ is the average radius and $2\bar{r}/3H$ is the added constant.

This geometrical model allows to determine the necessary shrinkage of the organic skeleton to obtain a desired interconnection size.

3.2. Morphological characteristics of sintered bodies

Fig. 9 represents structures obtained after debinding and sintering treatments undergone by the part for different values of shrinkage of organic frame.

The spherical pores present many interconnections with their neighbours. The interconnection size is adjusted by the shrinkage amplitude of the ball pile during the chemical-forming treatment and can vary from 0.2 to 0.6 times the diameter of the macropore, for limit values. These limitations are due to the low mechanical resistance of the organic scaffold when contacts between balls are small, to the difficulties in order to impregnate the polymeric skeleton by the casting slurry and to debind it when the building is too dense.

For the given example, PMMA balls used to build this organic skeleton were in a range from 600 to 700 µm. The interconnection diameter between pores varies from 110 to 280 µm for a shrinkage of the organic building from 90 to 3000 µm, respectively. The thickness of the ceramic walls decreases when interconnection size increases. This phenomenon is induced by an interpenetrating of the balls which increase with the sample shrinkage. Interstitial spaces between pores decrease and involve an increase of porous volume and consequently a reduction of mechanical properties. The porous volume of sintered material evolves from 65 to 80% for interconnection sizes from 110 to 280 µm, respectively (Fig. 10). Measurements carried out by

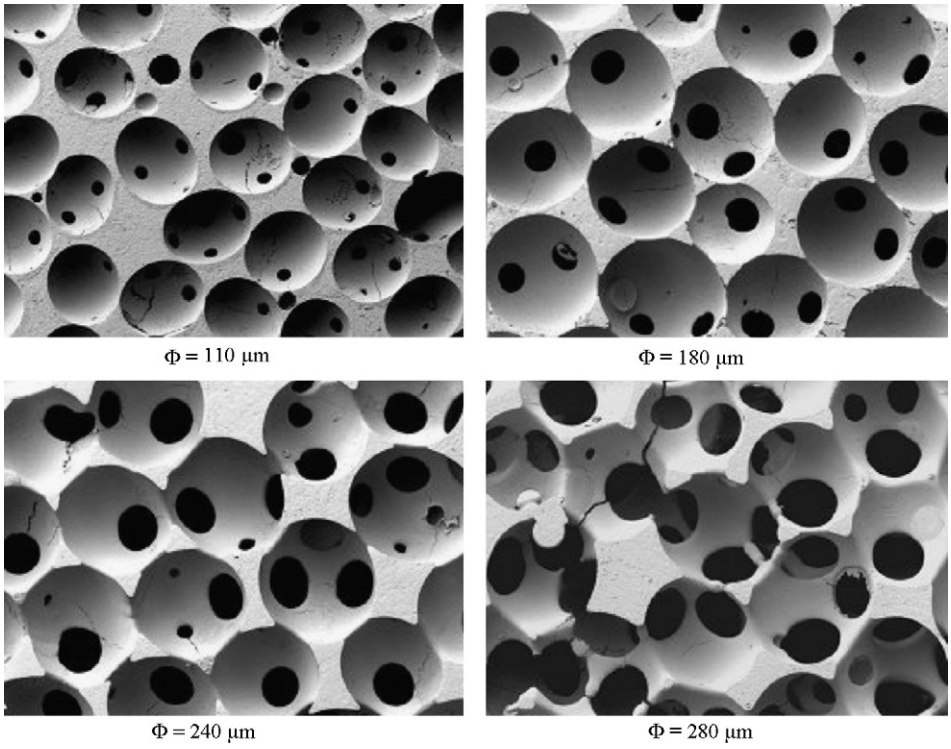

Fig. 9. Interconnection sizes of the pores according to the shrinkage of the organic building.

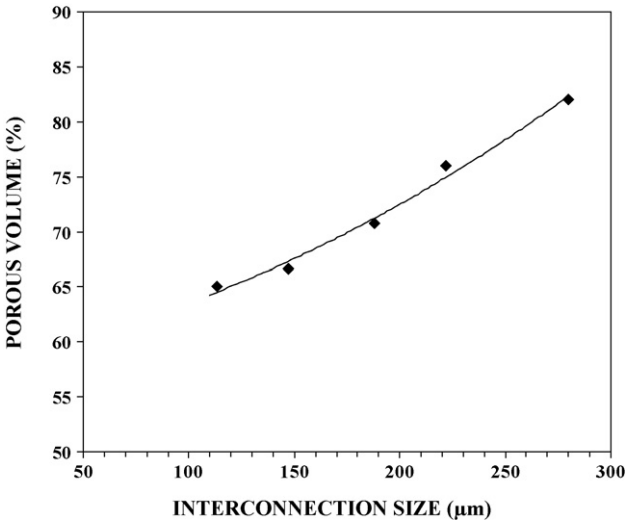

Fig. 10. Evolution of the porous volume as function of interconnection size of sintered ceramics.

mercury porosimetry confirmed that ceramics walls were free of open porosity with a relative density higher than 99%.

In addition to the control of the interconnection size, this new process allows to control the pore dimension by the initial choice of size of PMMA balls constituting the organic skeleton. Fig. 11 shows the macroporous ceramics carried out with diameter balls equal to (a) 100–200, (b) 300–400, (c) 500–600 and (d) 700–800 μm.

3.3. Applications

This new shaping process allows to easily carry out macroporous materials of varied forms and dimensions. In addition to, specific properties of material can be obtained and in particular parts with a gradient of pore sizes or a gradient of the interconnection sizes. In the first case, the gradient of the pore dimension is obtained by superimposing slices of PMMA balls with different diameters (Fig. 12). This ball pile is then connected by the action of ketonic solvent then, impregnated by the TCP suspension and thermally heated. In this example, the balls used successively have a diameter of 100–200, 400–500 and 700–800 μm.

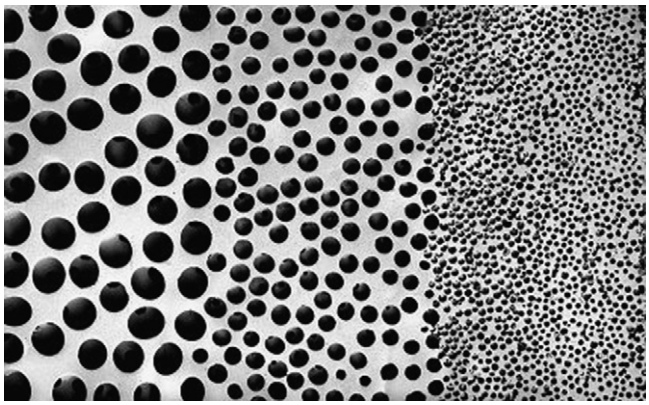

Fig. 12. Gradient of the pore size of sintered material.

In the second case, the gradient of the interconnection sizes is obtained by chemical forming of layers of PMMA balls piled up successively the ones on the others. A first layer of beads are connected during a time t_1, then is introduced into the mould a second layer of balls which undergoes this treatment of chemical forming during a time t_2 and so on.

Fig. 13 illustrates the size gradient of the interconnection on a sintered body obtained after a treatment of three layers of balls

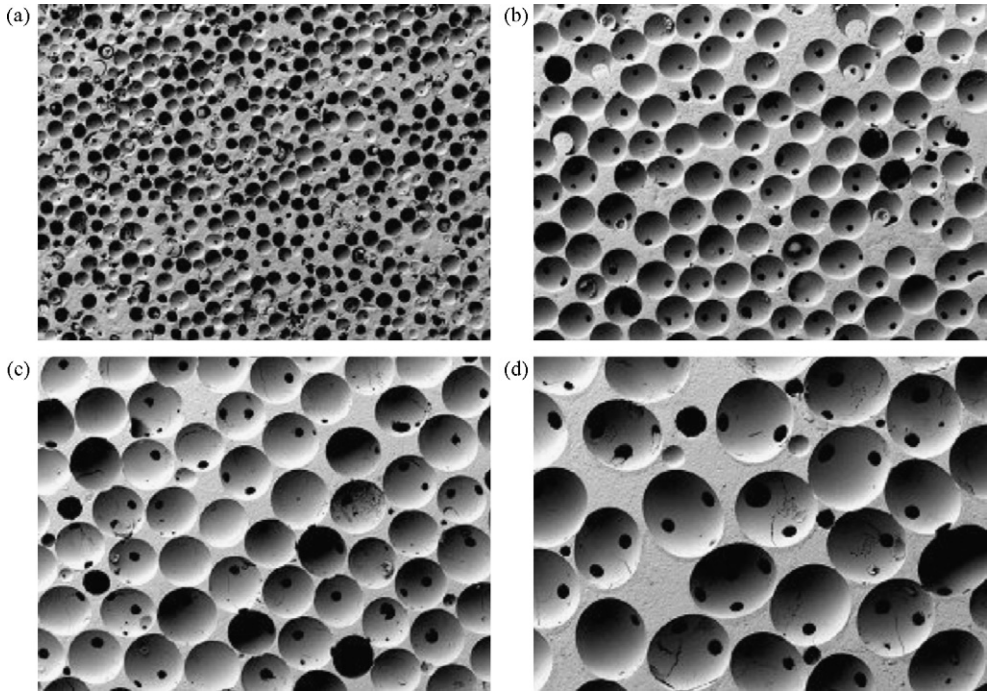

Fig. 11. β-TCP porous ceramics with different pore sizes.

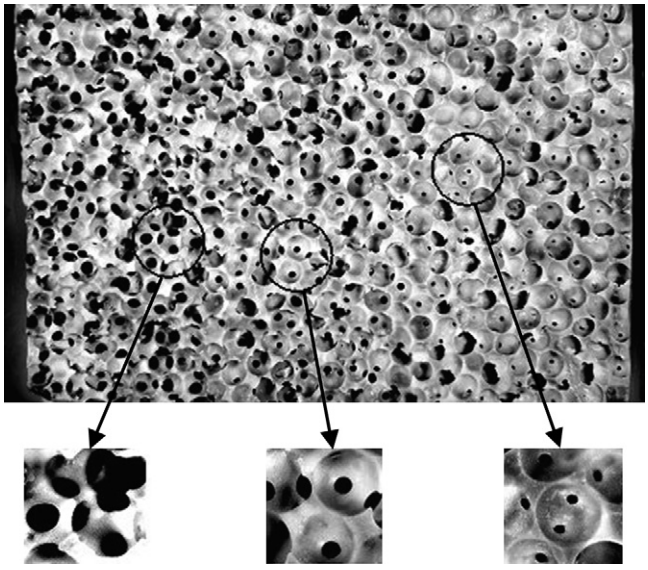

Fig. 13. Gradient of the interconnection size of sintered material.

of 600–700 μm. The treatment duration of these layers are equal to 90 min for the first layer ($t_1 + t_2 + t_3$), 30 min for the second layer ($t_2 + t_3$) and 10 min for third layer (t_3). Interconnection sizes vary from 110, 150 and 290 μm for the first, second and third layer, respectively.

These types of implant structure with a porous gradient and a sufficient degree of interconnection allow mimicking as much as possible the bimodal structure of bone (cortical and cancellous). Very porous portions allow the ingrowth of bone tissue and less dense portions allow a load bearing capacity similar to natural bone.

4. Conclusion

The optimal bone colonisation is very dependent of the porous characteristics of implant.

The new manufacturing process developed in this work authorises a total control of porous architecture of material and in particular of the pore size and their interconnectivity which conditions the clinical effectiveness of biomaterial.

This process allowed to obtain:

- A size of the spherical macropore which can vary from 100 to 900 μm.
- A controlled dimension of the interconnection between the pores which can extend from 0.2 to 0.6 times the pore diameter. An empirical study and a geometric model make possible to envisage the dimension of the contact between porogen particles which will constitute the future interconnections of sintered material.
- The realisation of material with a gradient of pore sizes or a gradient of the interconnection sizes.
- The manufacturing of net shaped parts without mechanical machining (free of pollution).
- An easily adaptation of the porous architectures, shapes and dimensions of body to the clinical application concerned.

The evaluation of mechanical properties of these materials are in progress. The first results obtained are interesting and indicate, for example, a compressive stress of about 18 MPa for samples with a average pore size of 600 μm, a interconnection size in range of 110 μm and a porous volume equal to 65%.

References

1. Burg, K. J. L., Porters, S. and Kellam, J. F., Biomaterial developments for bone tissue engineering. *Biomaterials*, 2000, **21**, 2347–3259.
2. Hench, L., Bioceramics. *J. Am. Ceram. Soc.*, 1998, **81**, 1705–1728.
3. Engin, N. O. and Tas, A. C., Manufacture of macroporous calcium hydroxyapatite bioceramics. *J. Eur. Ceram. Soc.*, 1999, **19**, 2569–2572.
4. Xie, Y., Biomatériaux hybrides innovants et leur évaluation in vivo. PhD Thesis. Université du Littoral Côte d'Opale, Boulogne, France, 2006.
5. Gauthier,. O., Bouler, J. M., Aguado, E., Pilet, P. and Daculsi, G., Macroporous biphasic calcium phosphate ceramics: influence of macropore diameter and macroporosity percentage on bone ingrowth. *Biomaterials*, 1998, **19**(1–3), 133–139.
6. Lu, J., Descamps, M., Dejou, J., Koubi, G., Hardouin, P., Lemaître, J. *et al.*, The biodegradation mechanism of calcium phosphate biomaterials in bone. *J. Biomed. Mater. Res. (Appl. Biomater.)*, 2002, **63**, 408–412.
7. Lu, J., Gallur, A., Flautre, B., Anselme, K., Descamps, M., Thierry, B. *et al.*, Comparative study of tissue reaction to calcium phosphate ceramics among cancellous, cortical and medullar bone sites in rabbits. *J. Biomed. Mater. Res.*, 1998, **42**, 357–367.
8. Hulbert, S. F., Klawitter, J. J., Leonard, R. b., Kriegel, W. W. and Palmours, H., ed., *Ceramics in Severe Environments*. Plenum Press, New York, 1971, p. 417.
9. Klawitter, J. J. and Hulbert, S. F., Application of porous ceramics for the attachment of load boring orthopaedic applications. *Biomed. Mater. Symp.*, 1971, **2**, 161–167.
10. Frayssinet, P., Trouillet, J. L., Rouquet, N., Azimus, E. and Autefage, Osseointegration of macroporous calcium phosphate ceramics having a different chemical composition. *Biomaterials*, 1993, **14**, 423–429.
11. Flautre, B., Descamps, M., Delecourt, C., Blary, M., Hardouin, P. and Porous, H. A., ceramic for bone replacement: role of the pores and interconnections-experimental study in the rabbit. *J. Mater. Sci. Mater. Med.*, 2001, **12**, 679–682.
12. Eggli, P. S., Mueller, W. and Schenk, R. K., Porous hydroxyapatite and tricalcium phosphate cylinders with two different macropore size ranges implanted in the cancellous bone of rabbits. *Clin. Orthop.*, 1998, **232**, 127–138.
13. Lu, J., Flautre, B., Anselme, K., Gallur, A., Descamps, M., Thierry, B. *et al.*, Role of the porous interconnections in porous bioceramics on bone recolonizatio*n in vitro* and *in vivo*. *J. Mater. Sci. Mater. Med.*, 1999, **10**, 111–120.
14. Liu, D. M., Fabrication of hydroxyapatite with controlled porosity. *J. Mater. Sci. Mater. Med.*, 1997, **8**, 227–232.
15. Jarcho, M., Calcium phosphate ceramics as hard tissue prosthetics. *Clin. Orthop. Rel. Res.*, 1981, **157**, 259–278.
16. Bucholz, R. W., Carlton, A. and Holmes, R. E., Hydroxyapatite and tricalcium phosphate bone graft substitutes. *Clin. Orthop.*, 1987, **18**, 323–334.
17. Rejda, B. V., Peelen, J. G. and de Groot, K., Tri-calcium phosphate as a bone substitute. *J. Bioeng.*, 1977, **1**, 93–97.
18. Ryshkewitch, E., Compression strength of porous sintered alumina and zirconia. *J. Am. Soc.*, 1953, **36**, 65–68.
19. Pollick, S., Shors, E. C., Holmes, R. E. and Kraut, R. A., Bone formation and implant degradation of coralline porous ceramics placed in bone and ectopic sites. *J. Oral. Maxillofac. Surg.*, 1995, **53**, 915–922.
20. Roy, D. M. and Linnehon, S. K., Hydroxyapatite formed from coral skeletal carbonate by hydrothermal exchange. *Nature*, 1974, **247**, 220–222.
21. Woyansky, J. S., Scott, C. E. and Minnear, W. P., Processing of porous ceramics. *Am. Ceram. Soc. Bull.*, 1992, **71**, 1674–1682.
22. Lelievre, F., Etude du coulage et du frittage de l'hydroxyapatite. Applications à la réalisation de pièces cellulaires. PhD Thesis. Faculté des sciences de Limoges, Limoges, France, 2006.

23. Tabaos, J. M., Maddox, R. D., Krebsbach, P. H. and Hollister, S. J., Indirect solid free form fabrication of local and global porous biomimetic and composite 3D polymer–ceramic scaffolds. *Biomaterials*, 2003, **24**, 181–194.
24. Descamps, M., Hornez, J. C. and Leriche, A., Effects of powder stoichiometry on the sintering of β-tricalcium phosphate. *J. Eur. Ceram. Soc.*, 2007, **27**, 2401–2406.
25. AFNOR, Designation NFS94-066. Détermination quantitative du rapport Ca/P de phosphate de calcium. Paris, AFNOR, 1998.
26. Raynaud, S., Champion, E., Bernache-Assolant, D. and Laval, J., Determination of calcium/phosphorus atomic ratio of calcium phosphate apatites using X-ray diffractometry. *J. Am. Ceram. Soc.*, 2001, **84**, 355–366.
27. White, H. E. and Walton, S. F., Particles packing and particle shape. *J. Am. Ceram. Soc.*, 1937, **20**, 155–166.
28. Scott, Packing of spheres. *Nature*, 1960, **188**, 908–909.
29. Rutgers, R., Packing of sphere. *Nature*, 1962, **193**, 465.
30. Berg, T. G. O., Mac Donald, R. L. and Trainor, R. J., The packing of spheres. *Powder Technol.*, 1969, **3**, 183.